[psfig,PASJadd]PASJ95kai

document

page1

Study of the Long-Term X-Ray Variability of a Possible Quasar RX J0957.9+6903 with ASCA

Yu-ichiro Ezoe[1], Naoko Iyomoto[2], and Kazuo Makishima[1] [12pt] [1]*Department of Physics, University of Tokyo, 7-3-1 Hongo, Bunkyo-ku, Tokyo 113-0033 E-mail(YE): ezoe@amalthea.phys.s.u-tokyo.ac.jp* [2]*The Institute of Space and Astronautical Science, 3-1-1 Yoshinodai, Sagamihara, Kanagawa 229-8510*

Long-term variability and spectral properties of a possible quasar, RX J0957.9+6903, were studied, utilizing 16 ASCA observations spanning 5.5 years. The average 0.7–10 keV spectrum of RX J0957.9+6903 is well represented by a power-law continuum of photon index 1.58 $\pm$ 0.03, and an absorption column of $\sim 1\times10^{21}$ cm^{-2}. The 2–10 keV flux of RX J0957.9+6903 varied by a factor of four over the period of six years, around a mean of $\sim 8.8\times10^{-12}$ erg s^{-1} cm^{-2}. Peak to peak variability within each observation was less than 25% on $\sim$ 1 day time scale. These properties support the classification of RX J0957.9+6903 as a quasar. The power spectrum density (PSD) was estimated in a "forward" manner, over a frequency range of $10^{-8.2}$–$10^{-4.3}$ Hz, by utilizing the structure function method and Monte-Carlo simulation assuming a broken power-law type PSD. Then, the break frequency $f_{\rm b}$ of the PSD of RX J0957.9+6903 has been constrained as $1/f_{\rm b} = 1600^{+\infty}_{-1100}$ days, and the logarithmic slope of the high-frequency region of the PSD as $\alpha = -1.55$ $\pm$ 0.2 . A comparison of the estimated PSDs is made between RX J0957.9+6903 and the M81 nucleus, observed in the same field of view.

Galaxies: active – Galaxies: individual (RX J0957.9+6903) – X-rays: galaxies – Methods: structure function

Introduction

Emission from an active galactic nucleus (AGN) is known to exhibit apparently random variability, over a wide wavelength range from radio to X-rays and γ-rays (e.g., Krolik et al. 1991; Edelson et al. 1996). Although the exact origin of such a variability is still unclear, it has been employed practically as a measure of the mass and size of the central black hole (BH) residing in the AGN. For example, Wandel & Mushotzky (1986) pointed out a strong correlation between the mass of the BHs in the AGNs estimated from optical emission lines, and the timescale of their X-ray variability in terms of the intensity doubling time. Hayashida et al. (1998) showed that the more luminous AGNs, which may have more massive central BHs, have longer timescale of variability; they utilized power spectrum density (PSD), which is mathematically more exact than the doubling time but suffers from the window function (the Fourier transform of the observational sampling) convolved with the true power spectrum of the source. These results indicate that the intrinsic X-ray variability timescale of AGN is an important parameter, which roughly represents the mass of the central BH.

Among AGNs, high-luminosity ones including quasars (QSOs) have such a long timescale of variability, e.g. a few years, that the analysis of their variability timescale needs long observations. Such long observations in X-rays are generally limited to the all-sky monitoring of bright sources, including a limited number of QSOs (e.g., > 30 mCrab for RXTE, where "1 mCrab" flux is $\sim 3 \times 10^{-11}$ erg s^{-1} cm^{-2} in the 2–10 keV range).

RX J0957.9+6903, a possible QSO, has been observed as many as 16 times over six years from 1993 to 1999 with ASCA, in which the total exposure time reaches 620 ksec. This is because the object lies close to the spiral galaxy M81, and was always within the same field-of-view (FOV) in the repeated ASCA observations of SN1993J. This object was first detected in the Einstein observation of M81, and was designated M81 X-9 (Fabbiano 1988; Elvis et al. 1992), although it is not associated with M81. Subsequently it was observed with EXOSAT (Giommi et al. 1991) and ROSAT, and renamed RX J0957.9+6903 (Bade et al. 1998). It was identified optically with a faint point-like object having an extreme blue continuum (Bade et al. 1998) in the wavelength range between 3400 Å and 5400 Å. These optical properties suggest that RX J0957.9+6903 is a QSO, even though its cosmological redshift is still unknown. On the other hand, its association with a possible supernovae remnant (SNR), at a separation of $\sim 10''$, was proposed from an H_α observation (Miller et al. 1995).

In the present paper, we first study the 0.7–10 keV X-ray spectrum of RX J0957.9+6903 and variability in section 3, and show them to be consistent with those of a QSO. We then analyze the long-term light curve of RX J0957.9+6903 more quantitatively in section 4, and estimate its PSD utilizing the new method, developed by Iyomoto et al. (2000) and Iyomoto (1999) to study the long-term variation of the M81 nucleus. Because RX J0957.9+6903 and the M81 nucleus have always been in the same ASCA FOV and observed under the same sampling window, we can directly compare the estimated PSD of these two objects, one being a promising QSO candidate while the other a typical low-luminosity AGN (LLAGN).

Observation

We observed the M81 region 16 times with ASCA as summarized in table 1. It is among the objects most frequently observed with ASCA. We analyze only data from the GIS (Gas Imaging Spectrometer; Ohashi et al. 1996; Makishima et al. 1996) with FOV of $50'$ diameter, because our target, RX J0957.9+6903, was always outside the SIS (Solid-State Imaging Spectrometer) FOV in even the 4-CCD mode ($22' \times 22'$ FOV). The GIS data were acquired in PH normal mode throughout.

For the GIS event selection, we required the geomagnetic cut-off rigidity to be > 8 GeV c^{-1} and the target elevation angle to be $> 5^\circ$ above the horizon. These criteria left us with 620 ksec of good GIS data. RX J0957.9+6903 was always detected, at a mean 0.7–10 keV counting rate of 6×10^{-2} c s^{-1} for each GIS detector (GIS2 or GIS3).

In figure 1 we show an example of the GIS images of the M81 region, after subtracting the non X-ray background. There were always two discrete X-ray sources in the GIS FOV; the brighter one (to the right in figure 1) is the emission complex from M81, while the fainter one (to the left in figure 1) is RX J0957.9+6903. The latter was detected at a J2000 position ($9^{\rm h}57^{\rm m}43^{\rm s}, +69^\circ04'03''$), which is consistent with the J2000 optical position ($9^{\rm h}57^{\rm m}51^{\rm s}{-}4pt.2pt0, +69^\circ03'30''$; Bade .et al. 1998) within the position accuracy of ASCA ($\sim 1'$; Tanaka et al. 1994). The M81 complex is elongated downward and upward because it consists of the nucleus (X-5) and three additional sources, SN 1993J, X-6, and X-4; these four sources are not resolved clearly from one another in the GIS image of figure 1. The results on SN 1993J have been reported by Kohmura (1994) and Kohmura et al. (1994). The results on the M81 nucleus of the 1st to 10th observations have been published as Ishisaki et al. (1996). The details of timing analysis of the M81 nucleus of all the 16 observations are published as Iyomoto et al. (2000).

X-Ray Properties of RX J0957.9+6903

Spectrum

For each observation, we accumulated photons within $3'$ of the X-ray centroid of RX J0957.9+6903 in the image and made spectra. The contamination from the M81 complex, estimated with the point spread function of the XRT (X-ray telescope), is less than $\sim 1\%$ of the total counts of RX J0957.9+6903 in this region, and can be negligible. Therefore, the background was taken from the same detector region in blank skies and subtracted, the count rate of which was an order of magnitude less than that of RX J0957.9+6903. The XRT+GIS response files were calculated separately for the two instruments (GIS2,3). We then added the GIS2 and GIS3 spectra into a single spectrum for each observation.

The obtained X-ray spectra of RX J0957.9+6903 are relatively featureless and all alike. In order to obtain a rough idea of the spectral variation, we fitted the 0.7–10 keV GIS (GIS2+GIS3) spectrum of individual observations with an absorbed power-law model. The absorption column density and photon index were taken as free parameters except the 16th observation. These 15 fittings were acceptable with the reduced $\chi^2 \sim 0.7$. The average absorption column density of these 15 spectral fittings was obtained as $\sim 9.5 \times 10^{20}$ cm^{-2}, which is higher than the Galactic line-of-sight column density of 4.06×10^{20} cm^{-2}. The average photon index turned out to be ~ 1.6 except the 13th observation, when the photon index was 2.2. For the spectrum of the 16th observation, the column density became lower than the Galactic value and therefore was fixed at that Galactic value, which yielded an acceptable fit. The 2–10 keV fluxes and photon indices derived in this way from individual observations are shown in figure 2a and figure 3, respectively, as a function of time.

Because the spectral variation is thus negligible except the 13th and 16th observations, we summed up all the GIS (GIS2+GIS3) data except the 13th and 16th into a single spectrum. We calculated the average XRT+GIS responses as averages of those for individual observations weighted by respective exposure times. We also calculated the average background. Using these response and background, we fitted the summed GIS spectrum in the 0.7–10 keV range with an absorbed power-law model. This model was acceptable with the reduced χ^2 of 0.92. The obtained best-fit model is shown in figure 4 and the best-fit parameters are given in table 2.

As shown in figure 4b, a similarly good fit (reduced χ^2 of 0.75) to the average spectrum has been obtained by replacing the power-law model with a bremsstrahlung model of temperature $kT = 12.0 \pm 0.8$ keV, with the absorbing column density fixed at the Galactic line-of-sight value. In table 2, we list these fit parameters as well.

Light curves

In figure 2a we present the background-subtracted long-term light curve of RX J0957.9+6903, in terms of the 2–10 keV flux as derived in section 3.1. Each data point corresponds to each of the 16 observations. Thus, the long-term variation amounts to a factor of $\sim$4 (peak-to-peak), around an average flux of 8.8×10^{-12} erg cm^{-2} s^{-1}.

To investigate the short-term variability, we subdivide each data point in the light curve into finer bins of 1/4 day width. Then, the peak-to-peak variation in each observation was found to be less than $\sim$ 15% except the 13th observation, when it was 25%. Figure 2b shows the short-term light curve of the 13th and 3rd observations, the latter being the longest one. With this bin size, all the 16 observations constitute a 51-bin light curve. Typical 1σ error due to photon counting statistics is $\sim$ 4% of the average flux, whereas root-mean-square (RMS) of overall variation through the entire light curve is much larger, 30% of the mean. This is important for our structure function analysis as described in section 4.1.

Comparison with the past observations

The flux of RX J0957.9+6903 measured in past observations is summarized in table 3. The results of the Einstein and EXOSAT data is quoted from Fabbiano (1988) and Giommi et al. 1991, respectively. The EXOSAT flux is converted from the countrate by utilizing the conversion factor in Fig 2 of Giommi et al. 1991. We extended the best fit power-law model of ASCA shown in table 2, to estimate the 0.2–4.0 , 0.05–2.0 and 0.5–2.0 keV fluxes. Below we explain the ROSAT data.

We newly analyzed the three ROSAT PSPC archive data in table 3, which cover epochs between the Einstein and ASCA observations. The background-subtracted PSPC spectra of RX J0957.9+6903 are show in figure 5. The background spectra were taken from the blank field in the same FOV of each observation. These spectra were represented by an absorbed power-law model with the photon index $\sim$ 2 and the absorption $\sim$ 2×10^{21} cm^{-2}. The reduced χ^2 were 9/13, 5/10, and 21/16 for the 1991 May, October, and 1992 September observations, respectively.

Compared with the estimated ASCA fluxes, the Einstein, EXOSAT and ROSAT values are lower by a factor of $\sim$ 1.5. Considering, however, uncertainties of the cross-calibration between different instruments operating in different bands, and the RMS = 30% of the ASCA light curve, these fluxes measured previously can be thought to be within the variation range of RX J0957.9+6903.

The nature of RX J0957.9+6903

We have for the first time measured an accurate 0.7–10 keV spectrum of RX J0957.9+6903, and derived short/long-term light curves. The obtained results, i.e., a power-law type spectrum with $\Gamma\sim1.6$, small short-term variability and a significant long-term variability, are consistent with the past suggestion of RX J0957.9+6903 being a QSO (Fabbiano 1988; Ishisaki et al. 1996; Bade et al. 1998). These hard spectra and the random variability over $\sim$ 6 years rule out the association of this object with an SNR (Miller et al. 1995). The object can not be a Seyfert galaxy since the optical counterpart is point-like (Bade et al. 1998). Although the featureless blue optical continuum is consistent with those of Blazers, the lack of a radio source within $\sim 1'$ of RX J0957.9+6903 (from NED) rules out its Blazer interpretation.

Although RX J0957.9+6903 has a high Galactic latitude ($\sim 40^\circ$), there still remains a small possibility that it is a Galactic object. The successful fit to the X-ray spectrum with a high-temperature Bremsstrahlung (figure 4b) leaves room for either a cataclysmic variable (CV) or a low-mass X-ray binary (LMXB); the former exhibits a genuine high-temperature thermal X-ray spectrum (e.g., Ishida 1991), while the latter an optically-thick spectrum which can be approximated by a mildly absorbed ($N_{\rm H}\sim1\times10^{21}$ cm^{-2}) high-temperature Bremsstrahlung (Makishima et al. 1989). The featureless blue optical continuum of RX J0957.9+6903 (Bade et al. 1998) is inconsistent with the CV interpretation, while consistent with the LMXB scenario where the optical emission mainly arises from reprocessed X-rays. However, in addition to the small number of high-latitude Galactic X-ray sources, its X-ray to optical flux ratio becomes log $[f_{\rm x}/f_{\rm B}]\sim0.9$ where $f_{\rm B}$ is the optical blue flux obtained from $m_{\rm B}$=18.6 (Bade et al. 1998). This is low for an LMXB which would show log $[f_{\rm X}/f_{\rm B}]\sim2-3$; e.g., Ritter 1990, while consistent with that of QSO (log $[f_{\rm X}/f_{\rm B}]\sim-1-+1$; e.g., Tananbaum et al. 1979).

From these considerations, we conclude that RX J0957.9+6903 is a radio-quiet QSO. If, for example, the object lies at a redshift of 1.0, the 2–10 keV luminosity becomes 3×10^{46} erg s^{-1}, assuming the Hubble constant to be 70 km s^{-1} Mpc^{-1} and a flat universe without cosmological constant. This is reasonable as a QSO luminosity.

Structure Function Analysis

We obtained a 51-bin light curve with the 1/4-day bin width. Because of the sparseness of this light curve, it is difficult to determine the PSD of RX J0957.9+6903 directly by Fourier transformation. Therefore we utilized the "forward method" analysis incorporating structure function as developed by Iyomoto (1999) and Iyomoto et al. (2000). Below we briefly explain this method. Further details of this method are given by Iyomoto et al. (2000).

Structure function For a time series of luminosity l_m, the first-order structure function (SF), $S(\tau_k)$, is given as

equation arrayrcl $\mathrm{S}(\tau_k) = 1N(\tau_k) \sum_{m=0}^{N-1-n} (l_m - l_{n+m})^2$

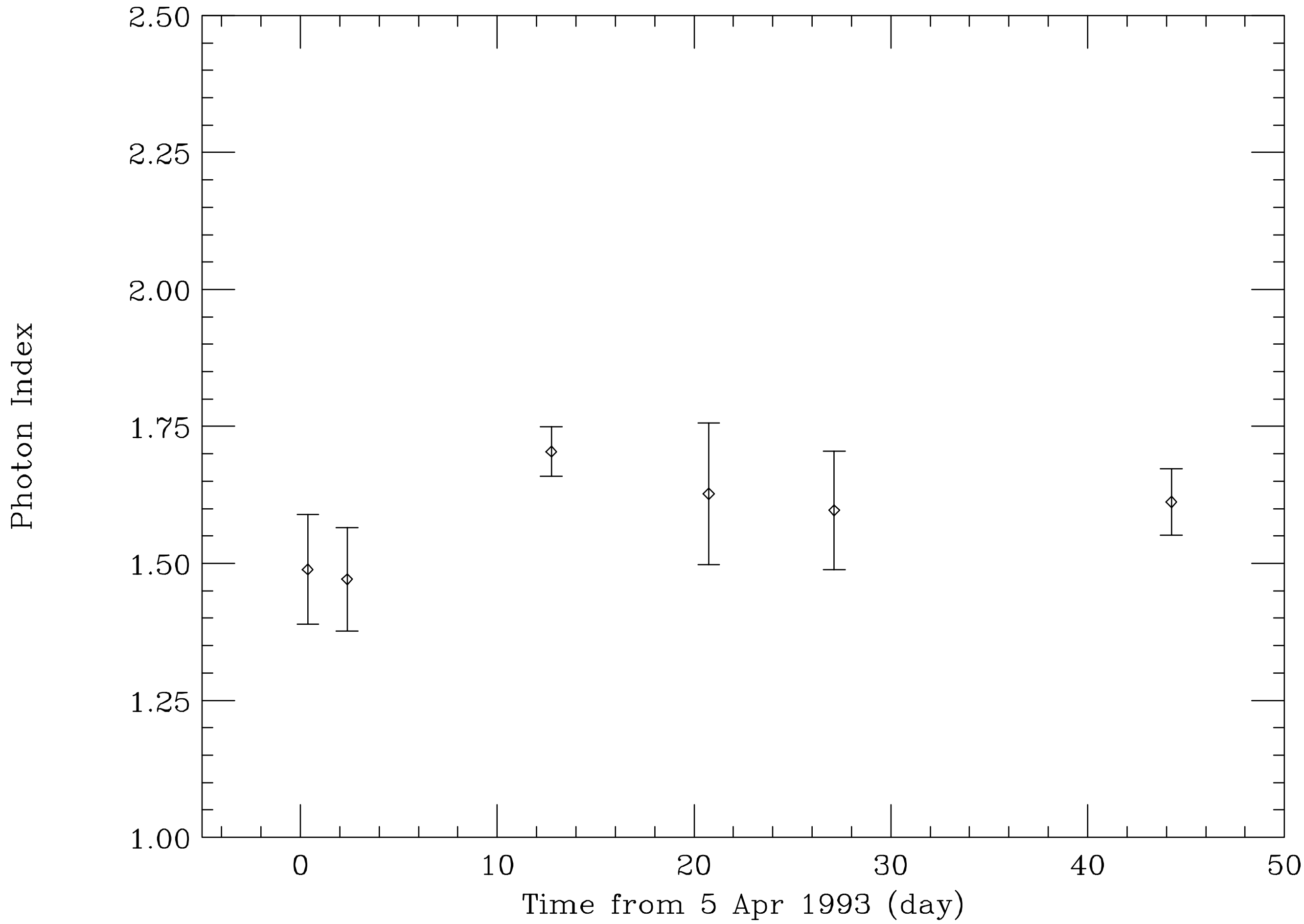

2.50
2.25
2.00
1.75
1.50
1.25
1.00
Photon Index
0
10
20
30
40
50
Time from 5 Apr 1993 (day)

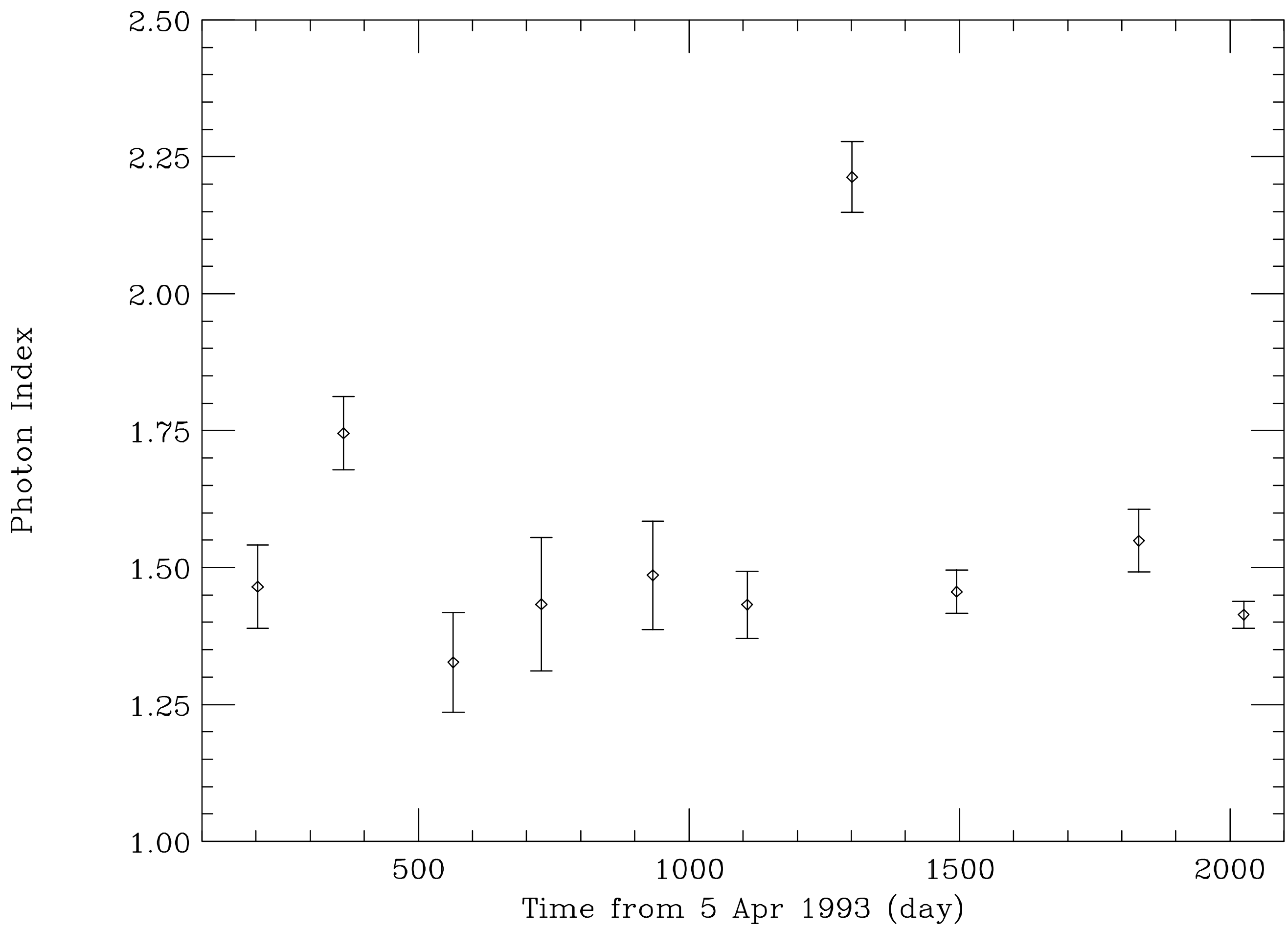

2.50
2.25
2.00
1.75
1.50
1.25
1.00
Photon Index
500
1000
1500
2000
Time from 5 Apr 1993 (day)